Engineering Model Development of HIBARI: MicroSatellite for Technology Demonstration of Variable-Shape Attitude Control

Kei Watanabe, Yuhei Kikuya, Kiyona Miyamoto, Tsuyoshi Nakashima, Teruaki Hayashi, Yoichi Okamoto, Naoki Kawaguchi, Hiroyuki Kobayashi, Soichi Sato, Shogo Nerome, Toshihiro Chujo, Yoichi Yatsu, Saburo Matunaga
Dept. Mechanical Engineering, School of Engineering, Tokyo Institute of Technology (which is same for all)
2-12-1, Ookayama, Meguro, Tokyo, 152-8552, Japan (which is same for all); +81 3 5734 2609
kwatanabe@lss.mes.tiech.ac.jp

ABSTRACT

We are developing a 40kg class microsatellite "HIBARI". The main technical mission is demonstration a novel attitude control method called "Variable Shape Attitude Control (VSAC)" proposed by Matunaga, Tokyo Institute of Technology. This VSAC is based on an idea to utilize a reaction torque generated by changing the shape of satellites, for example driving solar array paddles by actuators. HIBARI is planned to be launched in fiscal year 2021 under "Innovative Satellite Technology Demonstration Program" led by JAXA. We are developing EM of HIBARI and describes those in this paper. Specifically, the results of missions, systems, and various tests are shown and the validity is derived.

INTRODUCTION

In recent years, the number of micro/nano satellites and CubeSats has increased agility due to the miniaturization of electronic devices and the sale of dedicated components, and we can see a paradigm shift in the utilization of micro/nano satellites and CubeSats for various business and scientific purposes. The mission requirements have become more advanced, ranging astronomical observations, constellations and deep space exploration. However, there is a technical limit to the requirements that can be met by micro/nano satellites and CubeSats at present. This is especially noticeable in the attitude/orbit control systems and optics, because it is difficult to mount control moment gyros (CMG), propulsion systems and large observation systems due to limitation of volume and electric power. In order to solve this problem, it is necessary to make the on-board equipment multifunctional and further downsize. We pay attention to multi-functionalization, and are trying to realize a new control method to control the attitude/orbit by changing the shape of the satellite in orbit. We are trying to develop a new control method. The microsatellite HIBARI is an engineering mission satellite to demonstrate this control method in orbit. This satellite is currently under EM development and will be launched into earth orbit by JAXA "Innovative Satellite Technology Demonstration Program" in fiscal year 2021. This paper describes the mission, system and development status of the HIBARI variable geometry satellite.

VARIABLE SHAPE SYSTEM

By changing the system shape on the orbit, we can do following three main things.

(1) attitude control using anti-torque associated with shape change.
(2) Orbit/attitude control by changing external environmental forces such as atmospheric drag to achieve the target shape.
(3) Change of satellite function according to mission.

Figure 1 shows the concept of attitude control called VSAC (Variable Shape Attitude Control) in (1). The attitude of the satellite body is controlled by using part of the system (e.g. solar array paddle) as a rotary drive actuator. Since this method does not require motor drive at all times, it has better energy efficiency than conventional wheels. Also, by increasing the mass of the driving structure, the attitude change angle is increased, which enables agile attitude control and the inertia of the system is increased, which make stability control easier than before. In addition, by using control under non-holonomic constraints motion control, the attitude can be changed without changing the satellite shape. For example, in Figure 2, the attitude is slightly changed while restoring the shape by devising the driving order of the paddle. This makes it possible to change attitude of any 3 axes.

Figure 3 shows the concept of orbit and attitude control in (2). Generally, atmospheric resistance and solar radiation pressure are control disturbances. However, it is possible to control the orbit/attitude by paying attention to the fact that the amount and direction change depending on the system shape, and actively changing the shape and using these external forces. For example, it can be applied to de-orbit and formation flight utilizing atmospheric resistance in low earth orbit. Also, external torque can be used for RW unloading.

(3) can be applied not only to changing the observation mode due to deformation of the optical system, but also to thermal control due to changes in the sunshade and surface area. These will not be demonstrated on this satellite, but will be demonstrated on Transformable Spacecraft proposed by JAXA/ISAS and our next satellite.

In this satellite, the driving object for changing the shape is a solar array paddle with a power generation function, realizing a more multifunctional actuator. This will lead to system simplification, cost reduction, and mission diversification.

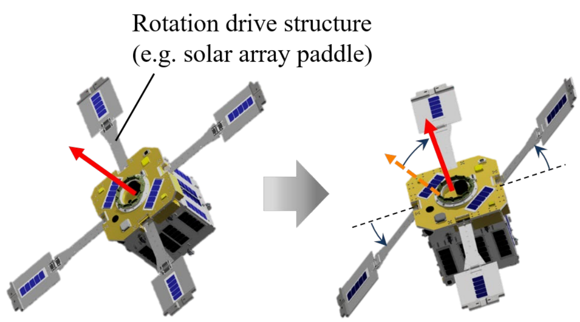

Figure 1: Concept of VSAC

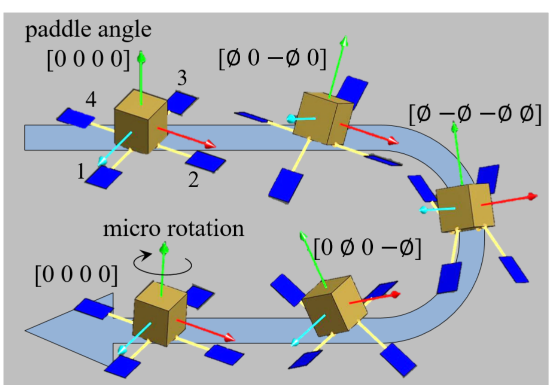

Figure 2: Example of Non-holonomic Attitude Control

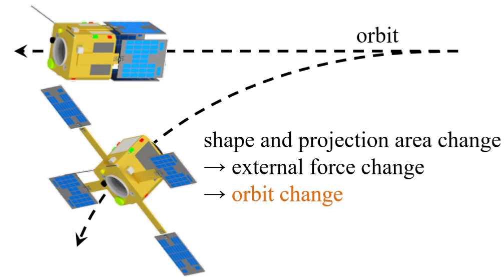

Figure 3: Orbit Control using External Force

MISSION DESIGN

Main Missions

We set the success criteria in Table 1 with the agile and large-angle VSAC demonstration as the main mission of HIBARI. In the minimum success, we confirm that the attitude changes actively by driving the paddles by motors.

At full success, we confirm the agility of VSAC. The performance target is 20deg/10sec. This is the performance equivalent to CMG for microsatellite.

In Extra Success, the objectives of VSAC performance evaluation are agile attitude change of 40deg/10sec, stable attitude control of 300arcsec/1sec, and large angle attitude change of 40deg or more using non-holonomic characteristics. In addition, stable control is performed in combination with RW, and the target is 300arcsec/10sec. This minute attitude change is detected by the blur of the star captured by the camera. In addition, we will also demonstrate orbit and attitude control using atmospheric resistance as a second stage operation.

Table 1: Success Criteria

Level	Mission
Min.	• Confirm attitude change predicted by variable shape function of motor drive
Full	• VSAC ◦ Agility: 20deg/10sec ◦ Pointing Accuracy: 5deg
Extra	• VSAC ◦ Agility: 40deg/10sec ◦ Stability: 300arcsec / 1sec ◦ Large-Angle Maneuver using Non-holonomic Control: 40deg • Cooperative control with RW ◦ Stability: 300arcsec / 10sec • confirmation of orbit/attitude change with controlled atmospheric resistance

Sub Missions

The following submissions are also conducted at HIBARI.

1. Attitude determination experiment using earth image and deep learning technology. We will apply the 3-axis earth sensor DLAS (Deep Leaning Attitude Sensor) that we have developed and demonstrated, and perform relative attitude estimation using continuous earth images.
2. Demonstration of UV imaging sensor for observation of gravitational wave objects
3. Demonstration of Nikon's consumer CMOS sensor.
4. Demonstration of real-time communication with the ground. Use the Globalstar Tx antenna "STINGR" for the ground.
5. Demonstration of a bus that basically complies with the CubeSat standard.

MODE OF OPERATION

Figure 4 shows the mode transition of HIBARI, and Table 2 shows the equipment used for each mode. The satellite first performs detumbling and spin-sun pointing using MTQ as critical modes. After establishing communication with the ground, we check out each device such as camera and RW. After that, the paddle is deployed while monitoring with a wide-angle camera. Since the development includes motor drive, it is positioned as a part of minimum success.

After the paddle is deployed, zero momentum sun pointing using MTQ is performed to prepare for the mission. In mission mode, first, VSAC only experiments are performed, and then cooperative experiments with RW are performed. These are carried out in the shade due to the requirement of STT accuracy and temperature stability. Also, when RW is driven, the geocentric orientation is set to the mission standby mode.

When power shortage or device anomaly is detected during operation, the satellite autonomously shifts to safe mode and performs processing according to the anomaly while pointing the sun.

Further, when the battery voltage becomes lower than the threshold value, the battery protection mode is entered. Power is cut off to areas other than the battery, and the attitude is uncontrolled.

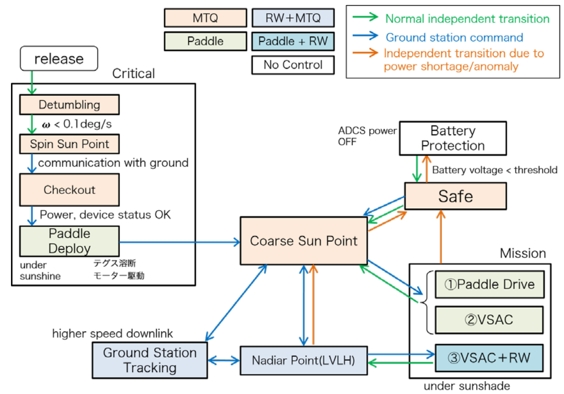

Figure 4: Mode transition diagram

Table 2: Equipment used in each mode

Mode		Sensor					Actuator		
		SAS (Sun Sensor)	GAS (Geomagnetic Sensor)	Gyro	STT (Star Tracker)	GPSR (GPS Receiver)	MTQ (Magnetic Toruque)	RW (Reaction Wheel)	Paddle
Critical	Detumbling		○	○			○		
	Spin up		○	○			○		
Nominal	① sun-pointing with MTQ spin-stabilization	○	○	○		○	○		
	② sun-pointing with RW 3 axis-stabilization	○	○	○	○	○		○	
Mission	① VSAC	○	○	○	○	○			○
	② VSAC + RW	○	○	○	○	○		○	○
Safe		○	○	○					

SYSTEM DESIGN

Figure 5 shows the HIBARI system diagram. The subsystem consists of the following: CDH (Command & Data Handling), COMM (Communication), ADCS (Attitude Determination & Control System), EPS (Electric Power System), and Camera system. Structure and Thermal.

A common MPU is placed in each subsystem, the inside of each system is monitored, and the CDH monitors each subsystem. By making the MPU common, development costs are reduced, defects are simplified, and the burden of CDH is reduced. Through the radiation test, this MPU has determined that there is no radiation failure.

Other equipment is basically selected based on radiation tests and on-orbit records. Most bus devices meet the CubeSat standard, and we are developing a standard bus applicable to CubeSat.

Figure 6 shows an external view of HIBARI. The paddle is folded to meet the loading requirements of the Epsilon rocket, and its size is 600 x 600 x 500mm. The satellite bus has a mass of 35 kg, and each paddle is 2.5 kg, and four are mounted.

The planned orbit is a sun-synchronous orbit with an altitude of 560 km and a descending intersection local solar time of 9:30.

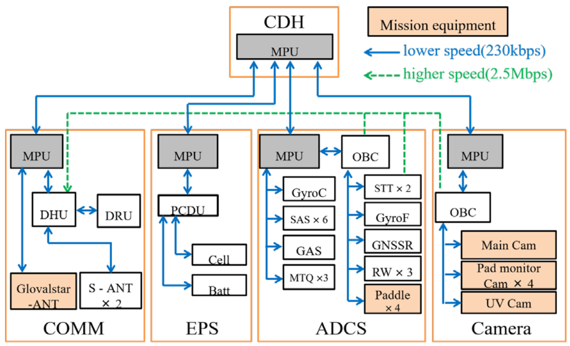

Figure 5: System Diagram

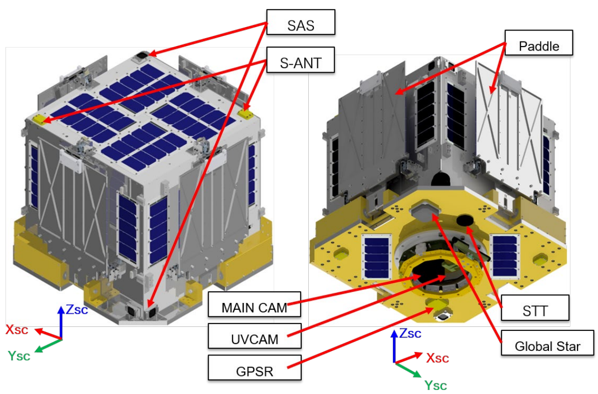

(a) Launch Configration

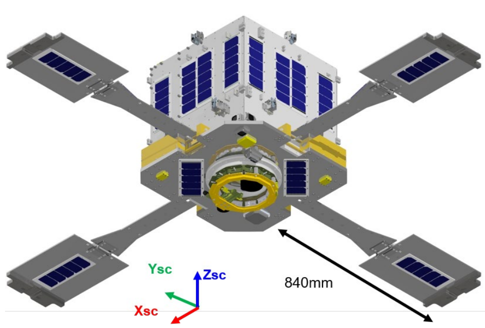

(b) On-orbit Configration

Figure 6: External View of HIBARI

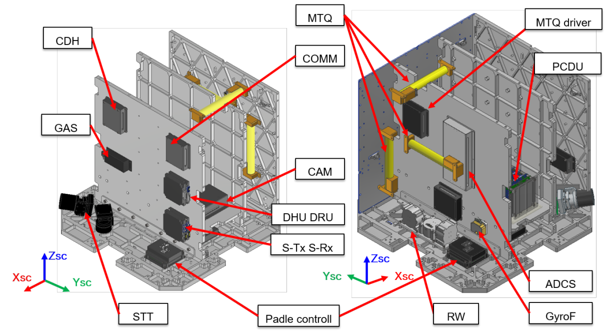

Figure 7: Internal Structure of HIBARI

Structure

The structural system is designed to meet the requirements for mass, center of gravity, rigidity, envelope area from rocket, and layout requirements for each device. Figure 7 shows the internal structure of HIBARI. Two parallel grid panels inside are used as load paths to fix many bus devices. As a result of the eigenvalue analysis, the machine axis direction is 45.7 Hz and the machine axis orthogonal direction is 86.5 Hz, which satisfies the rocket requirements. When the strength analysis of static load, sine wave, and random load was performed, the stress distribution was as shown in Fig. 8, and it was confirmed that the safety margin exceeded 0 in all cases.

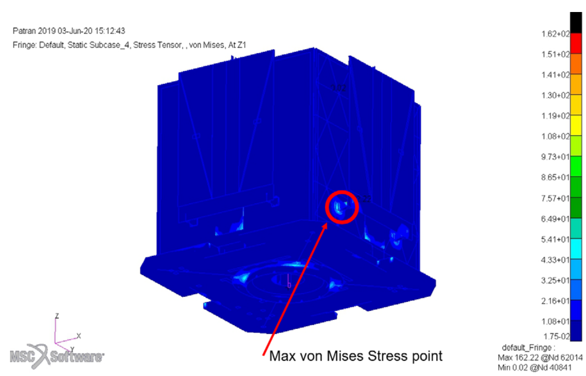

Figure 8: Strength Analysis

Figure 9 shows the internal structure of the paddle drive unit. The internal actuator is connected to the satellite structure while being housed in the box to protect it from the external environment. Furthermore, it is necessary to detect the rotation of the output shaft, including the backlash of the planetary gears, and determine the origin of the motor. Therefore, in addition to the motor control encoder, an absolute encoder is used on the output shaft side. As shown in Figure.10, the paddle is deployed by the hinge and motor drive.

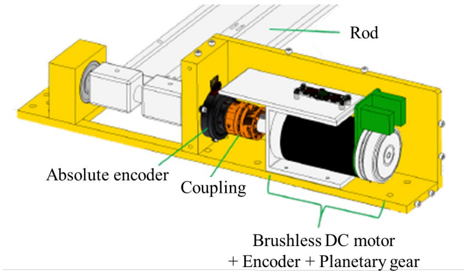

Figure 9: Paddle drive structure

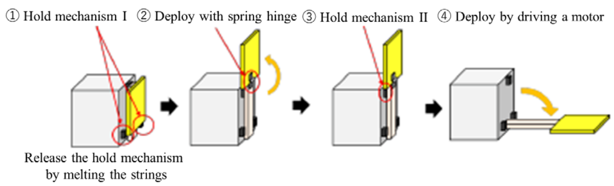

Figure 10: Paddle deployment sequence

Thermal

The thermal subsystem is designed to keep the temperature of the onboard equipment within the allowable temperature range. As a design policy, the temperature of the mounted equipment is designed not to exceed the allowable temperature range in the worst cold and hot cases. Table 3 shows the conditions for the worst cold and hot cases.

First, one-point analysis is performed to determine the thermal environment of the entire satellite, and the surface characteristics of the satellite enclosure are determined. Table 4 and 5 show the area ratios and surface characteristics of the constituent materials on each surface, which were determined based on the one-point analysis. The thermo-optical characteristics of the constituent materials used are shown in Table 6. Table 7 shows the results of a one-point analysis using the designed surface characteristics.

Next, in order to investigate the temperature environment of the onboard equipment with the surface characteristics designed by one-point analysis, thermal analysis is performed using Thermal Desktop. Figure 11 shows the analysis. Table 8 shows the allowable temperature range of typical onboard equipment and analysis results. The analysis results show that the temperature of the onboard equipment is within the allowable temperature range in the worst cold and hot cases. However, it can be seen that the battery temperature is low and the margin is small. In this analysis, the temperature environment was settled down in that case, and the battery was designed to be insulated from the surrounding structural materials, so the temperature was kept for a while when moving from the other case to the worst cold case. Since this is designed so that this result is acceptable.

Table 3: Analysis case conditions

item	Worst cold	Worst hot
Solar constant [W/m^2]	1318	1414
Albedo coefficient	0.2	0.4
Terrestrial infrared radiation [W/m^2]	261	189
β angle [deg]	35.0	37.5
Satellite average power consumption [W]	0.2	14.7
Attitude	Tumbling	Sun pointing

Table 4: Material area ratio on each side of the housing

Surface	solar cell	Alodine #1000	Black Kapton
Side panel	33.5 %	66.5 %	0 %
Sun pointing panel	69.6 %	0 %	30.4 %
Anti-sun pointing panel	11.3 %	88.7 %	0 %
all	34.1 %	61.1 %	4.8 %

Table 5: Surface characteristics of each side of the case

surface	α	ε	α/ε
Side panel	0.322	0.324	0.994
Sun pointing panel	0.715	0.859	0.832
Anti-sun pointing panel	0.222	0.149	1.48
all	0.361	0.369	0.979

Table 6: Thermo-optical properties of materials

	α	ε
Solar cell	0.625	0.85
Alodine #1000	0.17	0.06
Black kapton	0.92	0.88

Table 7: Satellite average temperature by single-point analysis

Worst cold [℃]	Worst hot [℃]
0.83	26.2

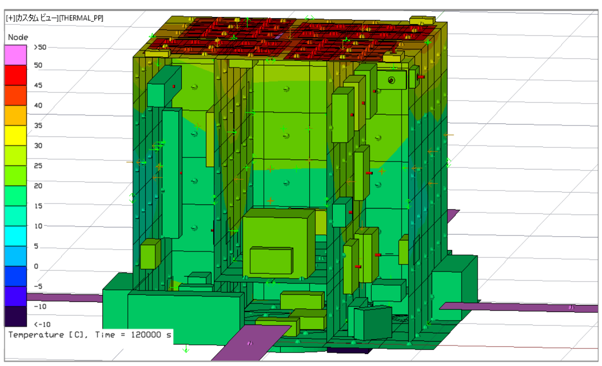

Figure 11: Thermal analysis

Table 8: Equipment allowable temperature

Onboard equipment	Allowable temperature [℃]	Worst cold [℃]	Worst hot [℃]
Battery	0~60	4.9~5.1	24.7~25.7
UV camera	-40~70	2.3~2.7	20.6~21.0
Gyro(F)	-40~85	-2.5~5.5	20.5~29.5

CDH&COMM

CDH collects and confirms HK (House Keeping) data of each subsystem, manages operation mode, and processes command and telemetry. The abnormality of each subsystem is detected from the HK data, and the operation mode is switched according to it. It also manages the satellite internal time and regularly synchronizes the time with each subsystem. Command/telemetry data is processed according to the flow shown in Fig. 12.

There are two types of communication devices, S band and Global Star communication. The S-band is a nominal communication system that receives commands from the ground and sends HK data and experimental data to the ground. Table 9 shows the line feasibility of S-band communication. The radiation pattern of the antenna depends on the satellite shape (described later), but a typical value is used here. For command reception and HK data transmission, in order to establish communication regardless of the attitude of the satellite, two transmitting and receiving antennas are installed so that the entire sky can be covered. Also, the receiver is always turned on so that commands can be received even when an error occurs. Since the transmission of experimental data is a high bit rate communication, ground station orientation is required. Global Star is used for simulation demonstration of real-time communication with the ground for future sudden astronomical observation.

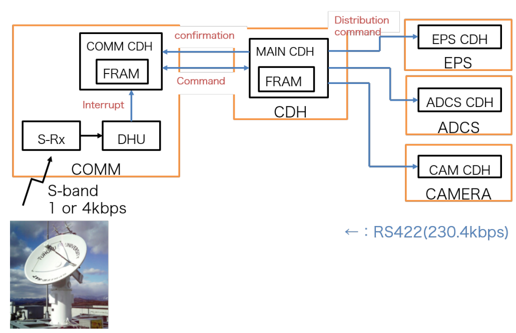

(a) uplink

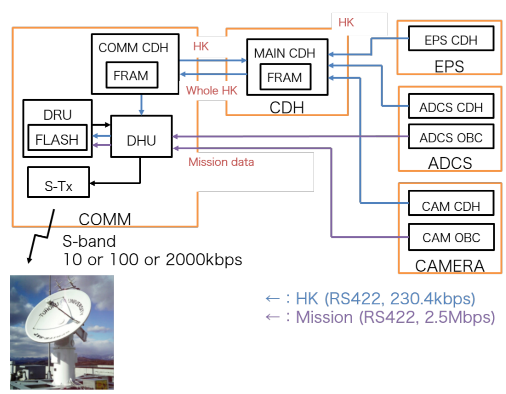

(b) downlink

Figure 12: Command/Telemetry data flow

Table 9: S-band link budget

item	Unit	Downlink	Uplink
Bitrate	kbps	100	1
Transmit Freq.	MHz	2285	2050
Transmit Power	mW	100	5000
Transmit Feed Loss	dB	-1	-7.6
Occupied Bandwidth	kHz	400	100
Max. Power Density	dBW/Hz	-66.0	-36.6
Transmit Antenna Gain	dBi	4.2	26.0
EIRP	dBW	-6.8	25.4
Orbital Height	km	560	560
Max. Comm. Distance	km	1315	2230
Elevation	deg	20.0	5.0
Transmission Loss	dB	-162.0	-165.6
Receive Antenna Gain	dBi	27.0	4.9
Receive Feed Loss	dB	-1	-1
Receive Signal Power	dBm	-112.8	-106.3
System Noise Temp.	K	250	750
G/T	dB/K	2.0	-24.9
Receive Noise Power Density	dBm/Hz	-174.6	-169.8
C/No	dBHz	61.8	63.6
Noise Bandwidth	dBHz	53.0	30
Req. S/No (Eb/No)	dB	4.4	9.6
Req. C/No	dBHz	57.4	39.6
Link Margin	dB	4.4	24.0

ADCS

The ADCS is composed of a coarse attitude system with a highly reliable MPU and a fine attitude system with an MPU capable of high-speed computation. Each device is purchased or developed as shown in Table 10. The coarse attitude system is used for backup of the precise attitude system when reliability is required more than the accuracy in critical mode or safe mode. The precise attitude system is used during missions where accuracy is required. Each of them performs attitude control processing as shown in Fig. 13, and is designed so that the coarse system functions as a backup even if the seminal system freezes or fails.

The data in ADCS is basically processed as telemetry via CDH, but a huge amount of data is acquired during a mission, so a high-speed communication line that can be directly sent to the COMM system is separately prepared (green line in Figure 5).

Table 10: ADCS Equipment details

Component	Where to prepare
GyroF	sensonor
GyroC	InvenSense
SAS	CubeSpace
GAS	Honeywell
STT	Self - developed
GNSSR	Chubu University
MTQ	NewSpaceSystem
RW	CubeSpace
Paddle	Self - developed

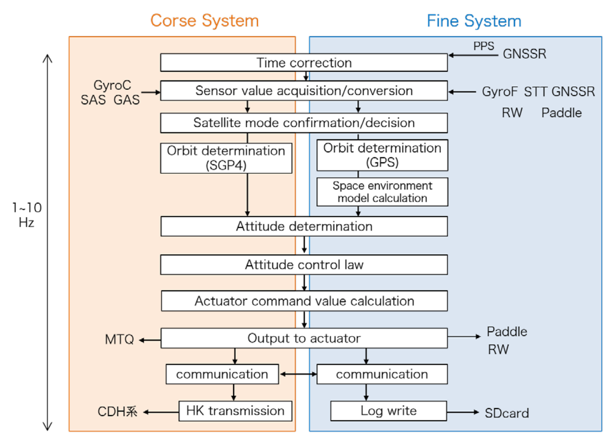

Figure 13: ADCSMain loop processing

EPS

EPS is responsible for system power management, power generation by solar cells and power management of batteries, appropriate supply of power to each device, and overcurrent detection. Table 11 shows the specifications of EPS.

Table 11: EPS Configuration

Description	Value
Peak Power Generation	53W
Battery type	Li-ION
Battery Configuration	2S7P
Battery Capacity	161Wh
PCDU Output Voltage	3.3V, 5V, 6.0-8.4V, 12V

Table 12 shows the power consumption by operation mode. Based on this table, solar cells are arranged on all sides of the satellite so that sufficient power can be generated when the sun is oriented, and that power can be generated in any attitude when in safe mode. By attaching solar cells to the drive paddle and monitoring the generated current, we confirm that the power from the actively driven paddle is input to the battery.

A battery of 161Wh is used so that the power will not be exhausted during the initial critical mode until the sun is supplemented or during the mission.

The PCDU controls the power generation from the solar cells, the charging/discharging of the battery, the power supply to each device, and prevents the overcharging and overdischarging of the battery. The PCDU monitors the current of the battery, output converter, and output port, and shuts off the current when an overcurrent flows.

The PCDU detects the overcurrent of the MPU of each subsystem, and the MPU of the system detects the overcurrent of the equipment in each subsystem, and is responsible for powering off and restarting.

Table 12: Power consumption in each mode

	Power consumption[W]					
	Detumblin g	Coarse sun pointin g	LVL H	Groun d station trackin g	VSA C	Saf e
CDH & COM M	5.4	5.4	5.4	11.1	5.4	4.5
ADCS	4.3	7.3	9.1	7.3	19.1	4.3
EPS	0.5	0.5	0.5	0.5	0.5	0.5
Camer a	0	1.1	1.1	1.1	9.8	0
Total	10.2	14.3	16.1	20.0	34.8	9.3

Camera

The camera system has three types of cameras; a main camera, a paddle monitor camera, and a UV camera. Table 13 summarizes each FoV (Field of View), number of mounted units, and applications. The main camera is used not only for earth observation, but also for star shooting for attitude stability evaluation. (Other specifications) Four paddle monitor cameras are integrated at the top of the satellite, and as shown in Fig. 0, the deployment and drive of the paddle can be photographed. In addition, by taking a picture of the earth, attitude determination using image identification, which is a submission, is also performed. The UV camera will be verified in orbit for future observations of gravitational wave objects.

Table 13: Camera system specifications

Camera	FoV[deg × deg]	Num ber	Usage
Main	8.2×5.4	1	• observation of the earth and astronomical objects • evaluation of attitude stability
Wide-angle	62.2×48.4	4	• capture paddle deployment and drive • determination of 3-axis attitude by using as earth sensor
UV	8.4×6.4	1	• Demonstration for future observation missions

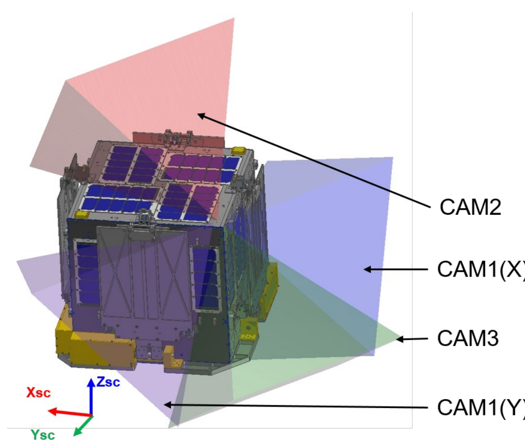

Figure 14: Paddle monitor camera FoV

TESTING

BBM Elec Integration Test

We conducted BBM electrical integration test by CDH system, communication system, EPS, ADCS. Figure 15 shows the situation during the test.

The following items were confirmed.

- Supply appropriate power from EPS to each subsystem device and operate for a long time.

- MPU of each subsystem can acquire HK data from each device

- CDH MPU can acquire and process HK data from each subsystem MPU.

- The HK data processed by CDH can be transmitted by COMM and received by the simulated ground station without loss.

- Simulated mission data can be transmitted from CAM-OBC to the ground station and received by the simulated ground station.

- CDH can receive the command sent from the ground station and send the command to MPU of each subsystem.

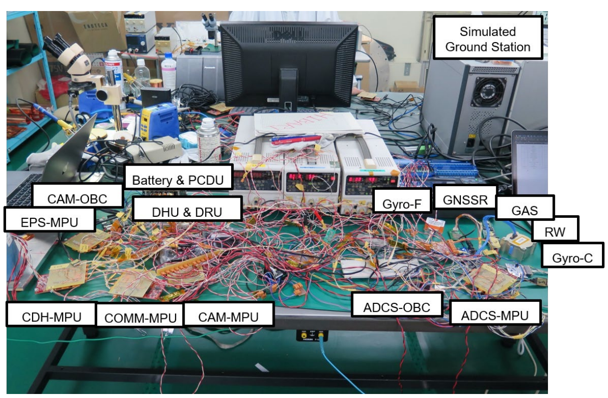

Figure 15: BBM test configurations

Paddle Deploy/Drive Test

A paddle deployment test using BBM was performed and it was confirmed that it could be deployed on the ground. In the deployment test, the effect of the weight of the paddle of the BBM cannot be ignored, so the paddle was hung with a texus for gravity compensation. During the test, the panel was folded by hand and then released. At this time, the rod is fixed. The time history of the deployment angle of the spring hinge was obtained by motion-capturing this behavior using OptiTrack. Figure 16 shows the appearance of the actual test at this time.

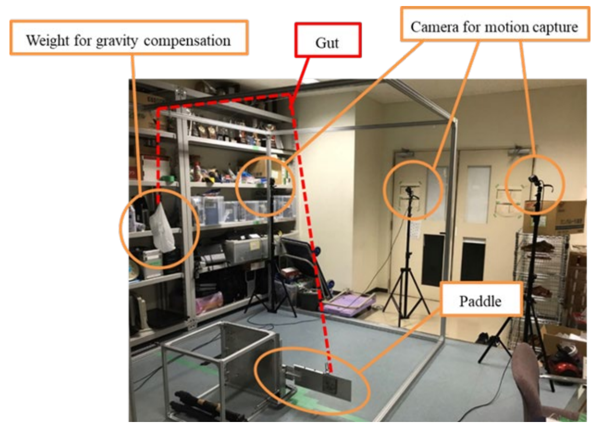

Figure 16: Paddle deployment test

Antenna Pattern Test

In HIBRI, the shield environment of communication radio waves fluctuates in orbit as the paddle is deployed and driven. Therefore, we measure antenna patterns according to various satellite shapes (paddle angles) and confirm that a sufficient line margin can be secured. Figure 18 shows the appearance of the test specimen. The paddle can simulate the shape before storage and after deployment (paddle angle 0deg, +90deg, -90deg). The antenna is mounted at a position corresponding to the actual configuration, and the radiation pattern is measured in an anechoic chamber.

As a typical measurement result, Fig. 19 shows the radiation pattern of the transmitting antenna when the paddle angle is 0 deg and +90 deg. Attitude angle represents the angle of deviation from the normal of the antenna mounting surface, and is measured on two planes, horizontal and vertical. In consideration of the line calculation, it was found that a line of 10 kbps communication was established in any attitude when the paddle angle was 0 deg, but it was found that it was established only in a limited range when +90 deg. .

This is because the paddle has a non-negligible effect as a radio wave shield. Since the angle is always +90deg when the paddle is deployed, it is necessary to make a design change so that the paddle does not act as a shield in order to secure a secure line, and it is currently under consideration. In addition, in other cases, it was confirmed that it is likely that a sufficient line would be established for both the uplink and downlink.

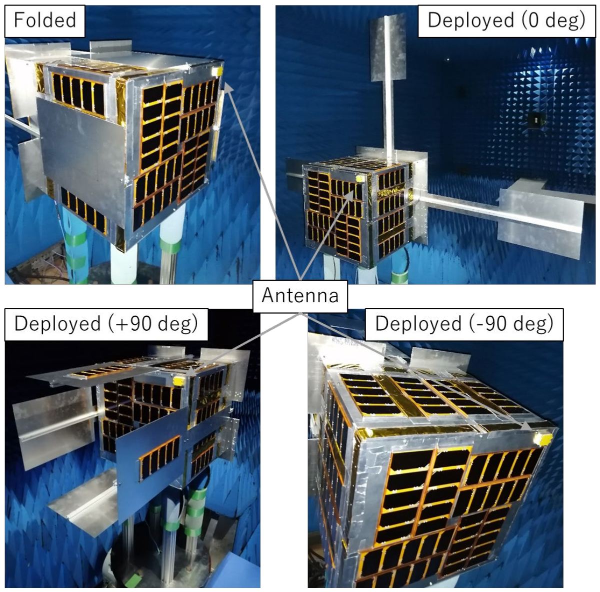

Figure 18: Antenna pattern test configurations

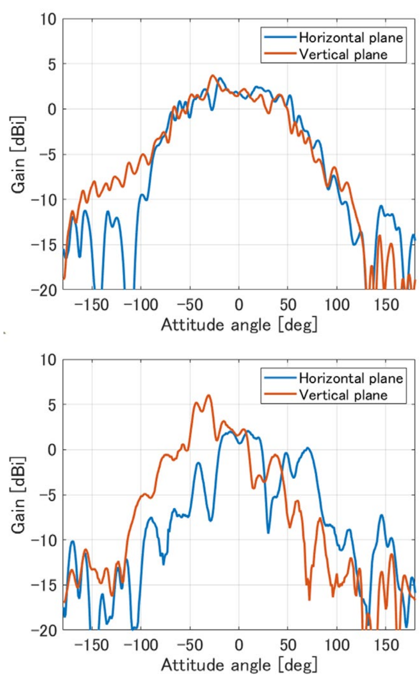

Figure 19: Antenna pattern test results of transmitting antenna (upper: deployed 0deg, lower: deployed +90 deg)

DEVELOPMENT PLAN

Figure 20 shows the development schedule. We are currently developing and testing EM.

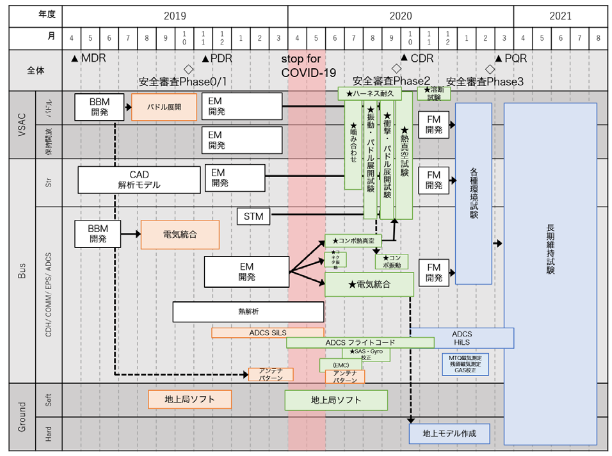

Figure 20: Development schedule

CONCLUSION

We are developing a 40kg microsatellite "HIBARI", which demonstrate a novel attitude control method called VSAC. This paper described the mission and system, various tests. HIBARI is planned to be launched within a few years. Currently in the EM development phase, we plan to develop FM this year.

ACKNOWLEDGMENT

This work was supported by JSPS KAKENHI Grant Number 17H01349 and MEXT space air commission expenses.

References

1. K. Tawara and S. Matunaga, "On Attitude Control of Microsatellite Using Shape Variable Elements," The 25th Workshop on JAXA: Astrodynamics and Flight Mechanics, Sagamihara, Japan, C-9, July 27-28, 2015.

2. K. Tawara, and S. Matunaga, "New Attitude Control for Agile Manoeuver and Stably Pointing Using Variable Shape Function and Reaction Wheels," The 26th Workshop on JAXA: Astrodynamics and Flight Mechanics, Sagamihara, Japan, July 2016.

3. K. Tawara, Y. Kikuya, N. Kondo, Y. Yatsud, and S. Matunaga, "Numerical Evaluation of On-Orbit Attitude Behavior for Microsatellites with Variable Shape Function," 67th International

Astronautical Congress (IAC), Guadalajara, Mexico, 26-30 September 2016.

4. K. Tawara, S. Harita, Y. Yatsu, S. Matunaga, and Hibari project team, “Technology Demonstration Microsatellite Hibari: Variable Shape Attitude Control and Its Application to Astrometry of Gravitational Wave Sources,” 31st International Symposium on Space Technology and Science, 2017-f-013, Matsuyama, Japan, June 3-9, 2017.
5. K. Sasaki, Y. Kikuya, S. Koizumi, Y. Masuda, Y. Shintani, T. Tsunemitsu, T. Furuya, Y. Iwasaki, Y. Takeuchi, K. Watanabe, Y. Yatsu, and S. Matunaga, “Variable Shape Attitude Control Demonstration with Microsat “Hibari”,” 32nd Annual AIAA/USU Conference on Samll Satellites, Utah, U.S.A, August, 2018.
6. Y. Shintani, T. Tsunemitsu, K. Watanabe, Y. Iwasaki, K. Tawara, H. Nakanishi, and S. Matunaga, “Preliminary Investigations on Ground Experiments of Variable Shape Attitude Control for Micro Satellites,” i-SAIRAS, Madrid, Spain, June, 2018.
7. Y. Kikuya, M. Matsushita, M. Koga, K. Ohta, Y. Hayashi, T. Koike, T. Ozawa, Y. Yatsu, and S. Matunaga, “Fault Tolerant Circuit Design for Low-cost and Multi-Functional Attitude Sensor Using Real-time Image Recognition,” 31st International Symposium on Space Technology and Science, 2017-f-093, Matsuyama, Japan, June 3-9, 2017.
8. Y. Kikuya, K. Sasaki, S. Koizumi, Y. Masuda, T. Ozawa, Y. Shintani, Y. Yatsu, and S. Matunaga, “Development of Low-cost and High Peformance Attitude Sensor applying Newral-network Image Recogniting Technology”, Proceedings of i-SAIRAS, Madrid, Spain, June, 2018.
9. S. Koizumi, Y. Kikuya, K. Sasaki, Y. Masuda, Y. Iwasaki, K. Watanabe, Y. Yatsu, and S. Matsunaga, “Development of Attitude Sensor using Deep Learning”, 32nd Annual AIAA/USU Conference on Samll Satellites, Utah, U.S.A, August, 2018.
10. Y. Iwasaki, Y. Kikuya, K. Sasaki, T. Ozawa, Y. Shintani, Y. Masuda, K. Watanabe, H. Mamiya, H. Ando, T. Nakashima, Y. Yatsu, S. Matunaga, “Development and Initial On-orbit Performance of Multi-Functional Attitude Sensor using Image Recognition,” 33rd Annual AIAA/USU Conference on Samll Satellites, Utah, U.S.A, August, 2019.